



Article

Ring-Shaped Surface Microstructures for Improved Lubrication Performance of Joint Prostheses

Philipp Drescher ^{1,*} , Paul Oldorf ², Tim Dreier ¹, Georg Schnell ¹, Rigo Peters ^{2,3} and Hermann Seitz ^{1,3}

¹ Microfluidics, Faculty of Mechanical Engineering and Marine Technology, University of Rostock, Justus-von-Liebig-Weg 6, 18059 Rostock, Germany; tim.dreier@uni-rostock.de (T.D.); georg.schnell@uni-rostock.de (G.S.); hermann.seitz@uni-rostock.de (H.S.)

² SLV Mecklenburg-Vorpommern GmbH, Alter Hafen Süd 4, 18069 Rostock, Germany; oldorf@slv-rostock.de (P.O.); peters@slv-rostock.de (R.P.)

³ Department Life, Light & Matter, University of Rostock, Albert-Einstein-Str. 25, 18059 Rostock, Germany

* Correspondence: philipp.drescher@uni-rostock.de; Tel.: +49-381-498-9118

Received: 10 March 2020; Accepted: 7 April 2020; Published: 9 April 2020



Abstract: The microstructuring of surfaces is a highly researched field that is aimed at enhancing the tribological behavior of sliding surfaces such as artificial joints, which are subject to wear. Lubrication of the joint interface plays a key role in the wear process, although the mechanisms of lubrication are quite complex. In order to improve the lubrication, the surfaces of the articulating components can be modified by pulsed femtosecond-laser microstructuring. Through microstructuring, the apparent dynamic viscosity of the synovial fluid between the artificial joint can be increased due to its non-Newtonian properties. This may lead to better hydrodynamic lubrication and, therefore, reduced particle abrasion. Femtosecond laser-induced microstructures were investigated in a modified rheometer setup featuring a reduced gap size in order to reproduce and measure the interface between fluid and implant surface more accurately. As a test fluid, a synovial fluid substitute was used. The study has shown that an increase in the viscosity of the synovial fluid substitute can be achieved by microstructuring. Compared to a smooth implant surface, the apparent viscosity of the synovial fluid substitute increased by over 30% when ring-shaped microstructures of 100 μm diameter with an aspect ratio of 0.66 were implemented.

Keywords: microstructuring; rheology; femtosecond laser; synovia; non-Newtonian fluids

1. Introduction

Three-body abrasion can result in aseptic loosening of endoprotheses and subsequently lead to a shorter life cycle, which represents the most common reason for revision surgeries of hip endoprosthesis. During a normal life cycle, the articulating surfaces of joint prostheses undergo different lubrication regimes, whereby mixed and full film lubrication is supported by the synovial fluid (SF). However, lubricant film in hip-joint replacements can be dysfunctional which can lead to three-body abrasion. Prosthetic joints usually consist of ultra-smooth bearing surfaces that are prone to abrasion, even though synovial lining tissue regenerates after implantation and provides sufficient lubricating fluid to allow the majority of joint replacements to function successfully [1]. The metallic debris and ions can then lead to an adverse reaction of the body [2]. Severe wear and aseptic loosening caused by wear particles are the main reasons that result in failure of such implants [3]. One approach to mitigate this problem is to improve lubrication of the articulating implant surfaces. Partial texturing, for example, is capable of generating significant load support and reducing friction. Many studies have investigated the texturing of surfaces in order to reduce friction [4] in technical applications such as bearings [5–7]

or other mechanical components [7–9]. The same principle can also be applied in the medical field, which is often subject to frictional load such as in artificial joints.

A study has shown that adding a micro texture to the smooth femoral component of a prosthetic knee joint reduces friction due to an increase of the lubricant film thickness between the bearing surfaces of the knee [10].

Research has already been carried out on the effect of different microstructures in endoprosthesis [11–13]. It is well known that hip joint bearings generally operate in a mixed, elastohydrodynamic lubrication regime. Therefore, a surface functionalization based on micro-structures may have a positive effect on the lubrication of hip endoprostheses and improve their wear resistance [13]. Results have shown that the use of laser-produced micro-pockets leads to a significant improvement in the lubricant film thickness compared with untreated surfaces [14]. A decrease in wear was also demonstrated on a metal on metal (MoM) hip endoprostheses with relatively large structures (in the range of millimeters), but with a limited scope of structure variations [15]. Textured steel surfaces showed a reduced friction coefficient against ultra-high molecular weight polyethylene (UHMWPE) in a pin-on-disc setup, regardless of the aspect ratio or the textured area density with dimple textures [16]. The use of dimple structures has also shown an improvement of tribological properties such as increased load-carrying capacity (LCC) and a greater electrohydrodynamic film, compared to ultra-smooth surfaces on CoCr/CoCrMo against UHMWPE [11,12]. Furthermore, it was also shown that wear decreased after multi-directional shear conditions in pin-on-disc tests of up to 50% (CoCrMo disc, against an HXPE (highly cross-linked polyethylene) pin). Additionally, electrochemical measurements outlined that the textured surfaces (dimple design) did not affect the corrosion potential of the metal-on-polyethylene (MoP) bearing [17]. It can also be added that these textures can act as wear traps for particles and subsequently improve the life cycle of artificial joints [18–20].

However, investigations were carried out with a Newtonian fluid and are, therefore, not comparable to *in vivo* conditions. This study aims to improve the investigations by using a non-Newtonian fluid in order to depict a more physically accurate model. Since synovial fluid is of limited supply, fluids with similar properties can be used as a substitute. Extensive research has been carried out to investigate synovial fluid and to develop synovial fluid substitutes that exhibit the same rheological properties [21–25]. This study uses a synovial fluid substitute (SFS) that exhibits similar behavior to healthy human synovial fluid.

Most research has investigated the effect of dimple structures in regard to the measurement of the friction coefficient and lubricant film thickness or rather the hydrodynamic pressure. However, microstructures can also have an effect on the viscosity of the synovial fluid, which plays an important role in the maintenance and adjustment of the lubricant film and, therefore, the performance of the hydrodynamic lubrication. Classical elastohydrodynamic (EHL) models are used to predict film thickness and the resulting performance in joint endoprostheses [26]. However, one of the key findings was that the lubricant film thickness does not obey EHL rules [27]. It was concluded that film thickness could not be predicted by using the rheology of simple Newtonian fluids in steady state contact conditions. Instead, interfacial film formation was determined by local rheological changes in the contact area and is driven by an aggregation of proteins within the contact inlet region [28,29]. Surface textures, for example, are discontinuities in film thickness that exhibit complex and transient load and kinematic multi-axis cycles. Despite extensive research, the wear of the bearing surfaces, especially the metal-metal hip endoprostheses, remains a major problem. Relatively little is known about the lubrication mechanisms prevailing in artificial joints, which still represents a serious gap.

An investigation on the impact of microstructures on the viscosity of a non-Newtonian lubricating fluid is carried out. Microstructuring of implant surfaces with a pulsed laser has become more common in recent years since it shows great promise in creating well-defined microstructures, improving mechanical properties and wear resistance [12,30] without introducing significant thermal effects [31,32]. Many aspects like laser parameters, structure geometry and texture density need to be considered in order to find beneficial effects [8]. The discovery of such optimized parameters in regard to improved

mechanical, tribological and rheological properties is still an ongoing process [7,33,34]. In this study, the lubrication performance is evaluated by measuring the dynamic shear viscosity of the lubricant with a parallel plate setup on microstructured specimens and an unstructured reference specimen. However, since the surface of the specimen does not consist of a smooth surface due to the microstructuring, the real dynamic viscosity η is not measured. Instead, an apparent dynamic viscosity η' is introduced that describes the interaction between the fluid and microstructured surface interface and also considers the non-linear relationship between shear rate and shear stress of non-Newtonian fluids. A new test setup was used that is able to determine the rheological properties of the non-Newtonian lubricant in small gaps. Measuring the viscosity in small gaps has many advantages such as enabling higher shear rates or the necessity of less test fluid [34]. This also possibly enables a closer investigation of the effect of microstructures on the non-Newtonian lubricant fluid. In a previous study, it was shown that the use of various microstructures had an improving effect on the apparent viscosity of a synovial substitute [33]. The aim of this study is to help to better understand the underlying mechanics of structural parameters in regard to their viscosity enhancing effect and help evaluate the impact of microstructured surfaces on the lubrication performance.

2. Materials and Methods

2.1. Specimens

The disks for the laser structuring and the subsequent apparent dynamic viscosity measurements have a diameter of 25 mm and a height of 6 mm with an average surface roughness of $Ra \leq 0.1 \mu\text{m}$ of the initial smooth surface. The material is a medical CoCrMo alloy type Ergiloy 9.9135HL from the company Zapp Precision Metals GmbH (Ratingen, Germany). Dimensions of the structuring area on the samples are given in Figure 1, with d as the microstructure's diameter, t as the microstructure depth, w for the microstructure distance and a for the microstructure's width.

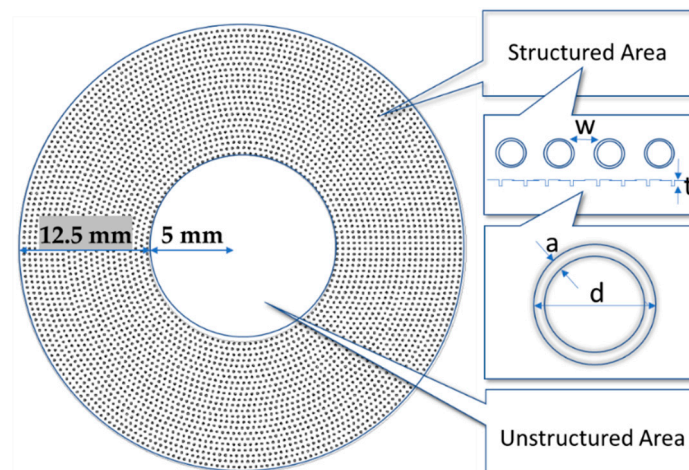


Figure 1. Schematic representation of a microstructured disk sample for the rheological investigations. An unstructured area was kept in the center of the parallel plate setup where only low shear rates occur.

2.2. Micromachining and Surface Characterization

Micromachining was carried out with a femtosecond fiber laser of the type TruMicro 5050 Femto Edition (Trumpf GmbH & Co. KG, Ditzingen, Germany) and a pulse duration of 800 fs. A ring area of the disks with an outer radius of 12.5 mm and an inner radius of 5 mm was microstructured (see Figure 1) using a galvo scanner of the type intelliSCAN 14 (Scanlab GmbH, Puchheim, Germany) including a F-Theta lens with a focal length of 82 mm. To achieve high structure quality with smooth edges and to avoid burr, a low fluence of 0.95 J/cm^2 and a repetition rate of 50 kHz were used. Some process parameters had to be optimized considering the geometry of the microstructure. Small adjustments

such as pulse overlap or scanning strategy were, therefore, carried out in order to obtain the best results for the structuring with negligible thermal influence. For optimized structures, a scanning speed of 200 mm/s and a pulse overlap of about 65% were set. After structuring, the samples were ultrasonically cleaned in deionized water. The diameter of the microstructured rings are 100 μm with different aspect ratios leading to a total of nine different microstructures. These microstructures were chosen because they showed the best results in a previous study with different promising microstructures such as squared dimples [7] or various net structures [33]. Further details of the implemented microstructures, depicted in Figure 1, are given in Table 1. The surface structure in regard to depth, lateral distance and gap width was measured at least three times at a magnification of 10 \times and 50 \times , using a laser scanning microscope (VK-X200, Keyence Corporation, Osaka, Japan).

Table 1. Specifications of the ring-shaped microstructures.

ID	Lateral Distance w (μm)	Gap Width a (μm)	Gap Depth t (μm)	Aspect Ratio (-)	Texture Area Density (%)
S1	300	15	20	1.33	2.6
S2	200	15	20	1.33	5.9
S3	150	15	20	1.33	10.5
S4	300	15	10	0.66	2.6
S5	200	15	10	0.66	5.9
S6	150	15	10	0.66	10.5
S7	300	15	5	0.33	2.6
S8	200	15	5	0.33	5.9
S9	150	15	5	0.33	10.5
Ref	-	-	-	-	-

2.3. Rheological Setup and Determination of Viscosity in Thin Gaps

For measuring the viscosity, the rheometer MCR 702 with its software RheoCompass (Version 1.20.493) from the company Anton Paar Germany GmbH (Ostfildern, Germany) was used. In order to be able to measure the effect of the microstructures, the device-specific gap between the specimens and the measurement geometry was reduced from 500 μm to 100 μm . The gap reduction was realized by customizing the rheometer MCR 702 with a test setup so a more precise measurement of the impact of the microstructures to the fluid can be carried out.

To ensure the parallelism and adjust the alignment of the 100 μm parallel plate test setup, an adjustable lower stainless-steel plate (alignment adapter) and two ferromagnetic steel plates as signal amplifiers (Figure 2a) were used. The setup uses three adjustable micro screws and a resonant inductive sensor for measuring and adjusting the distance between the two steel plates. Before the small gap is implemented, the zero point is determined by lowering the upper plate until it hits contact with the lower plate. The same procedure is carried out with the modified setup. After parallelism was achieved, the steel plates need to be removed and the specimens inserted and fixated in the corresponding alignment adapter (Figure 2b) and the new zero point is determined. With this setup, the gap between both plates can be reduced and a high parallelism realized. Figure 2 shows the setup of the samples with the sensor and the micro screws.

The gap between the plates was measured relatively with the use of an inductive sensor by building a small resonant circuit. The sensor measures the change of the inductivity. The frequency changes were quantified with a frequency counter 53131A (Keysight Technologies, Santa Rosa, CA, USA). By relocating the sensor and adjusting the screws, the same frequency on all locations of the sensor on the plate could be achieved, meaning that the gap between the plates was equal with a certain margin of error ($\pm 5 \mu\text{m}$). Figure 2a shows the adjustment of the gap with the use of the inductive sensor. A complete revolution of the screw by 360 $^\circ$ corresponds to a height shift of the plate of 100 μm . With the precision adjustment screws it is possible to achieve a frequency change of 0.6 MHz with one complete revolution. The resolution of the frequency counter is high enough to measure small changes

in the frequency and, therefore, the height of the plate by approx. 5 μm . After the alignment has been carried out, the sensor is removed and the structured specimen can be inserted into the corresponding pocket in the alignment adapter and fixated with an Allen screw.

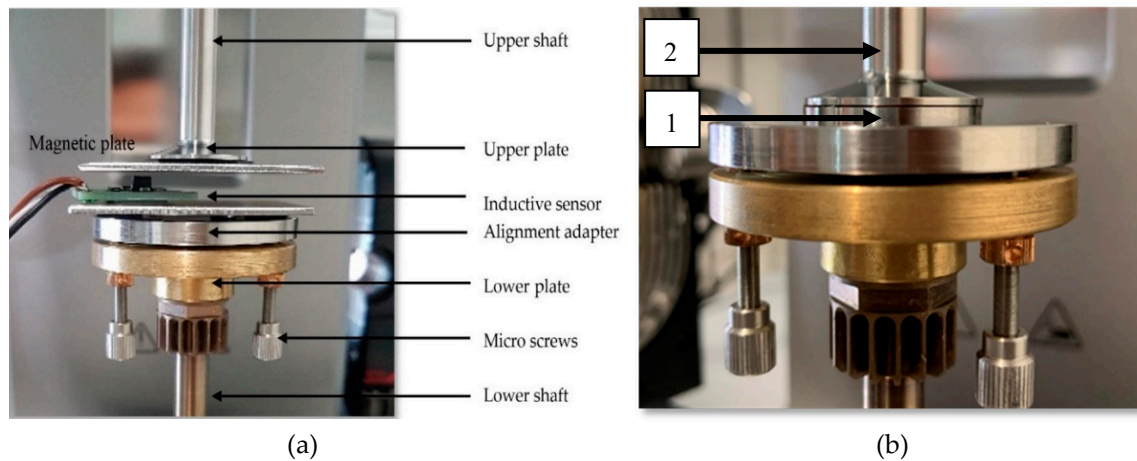


Figure 2. Custom rheological setup (a) of the adapter and measurement of the alignment of the two parallel plates before rheological testing; (b) final setup with the microstructured sample (1) in the commercial rheometer system MCR 702 with the unstructured $\text{Ø}25\text{ mm}$ measurement geometry (2).

The measurements of the apparent dynamic viscosity were carried out at a room temperature of 20 $^{\circ}\text{C}$ and at a constant shear rate of 100 s^{-1} , even though a shear rate dependency of the viscosity of joint fluid is well known [21,24]. Nonetheless, it was necessary to measure the properties in the chosen range in order to effectively compare the samples to each other. For validation, the test setup was used to measure the viscosity of distilled water and consecutively a non-Newtonian fluid. Instead of using synovial fluid, a substitute fluid exhibiting comparable non-Newtonian behavior was used. The test fluid was applied with the pipette VITLAB[®] micropipette (VITLAB GmbH, Grossostheim, Germany). The non-Newtonian SFS test fluid, in accordance with ISO 14242-1 [35], consists of a fetal bovine serum from the company Capricorn Scientific GmbH (Ebsdorfergrund, Germany) with a total protein content of 3.7 g/dL, including an albumin and γ -globulin content of 2.1 g/dL and 136 mg/dL, respectively. Hyaluronic acid (HA) with a molecular weight of 2×10^6 Da was added with a ratio of 3 g/L in order to achieve the same range of viscosity as normal synovial fluid [22], which has a concentration of HA in the range of 2%–3% with a molecular weight of 10^6 – 10^7 Da [36]. The HA was purchased from the company Sigma-Aldrich Chemie GmbH (Taufkirchen, Germany). The viscosity of the fluids was measured with the rheometer MCR 702 and calculated using the following equations:

$$\eta' = \frac{\tau_{corr}}{\dot{\gamma}_c} \text{ and } \tau_{corr} = \frac{\tau}{4} \left(3 + \frac{dM}{d\dot{\gamma}_c} \right) \quad (1)$$

with η' as the apparent dynamic viscosity, τ as the shear stress, M as the momentum and $\dot{\gamma}_c$ as the velocity gradient. The shear stresses for non-Newtonian fluids obtained using parallel plates must be corrected using the widely known Weissenberg–Rabinowitsch correction. However, since this equation is only used on smooth surfaces, this apparent dynamic viscosity further describes the rheological behavior of the fluid in the interphase between the fluid and a structured surface.

Nine specimens with different microstructures (see Table 1) as well as an unstructured specimen for reference were investigated in regard to their effect on the apparent dynamic viscosity of the SFS. Focus was maintained on the effect of different texture densities and aspect ratios on the rheological behavior. For validating purposes, distilled water was also measured with the newly designed test setup. The effect of HA on the SFS was also measured using bovine serum with and without HA.

The apparent dynamic viscosity on each sample was determined at least three times for statistical reasons. All data are expressed as means \pm standard deviation. A two-factor analysis of variance (ANOVA) was performed to statistically examine significant differences between the means with a confidence interval of $CI_{.95}$. A significance level of $*p < 0.05$ was considered as statistically significant. The interrelationship and statistical analyses among the means of aspect ratio and texture area density consisting of three different variations, were assessed using Excel 2016 (Microsoft, Redmond, WA, USA).

3. Results

Microstructuring of CoCrMo disks was carried out successfully using a femtosecond laser, as shown in Figure 3a. As seen in Figure 3b,c, optical and profilometric analysis shows well-defined and sharp structures without any unwanted debris or deformations. Due to the Gaussian beam of the ultrashort laser pulses, the microstructures show a typical laser-generated groove profile with high qualities and a minimized burr, resulting in a width of $a = 14.9 \pm 1.3 \mu\text{m}$. The standard deviation of the ring depth is $t = 20 \pm 0.9 \mu\text{m}$.



Figure 3. Microstructured CoCrMo sample. (a) Sample with global geometrical dimensions of the structured area. (b) Microscopic illustration of ring structure with diameter of 150 μm , gap width of 15 μm and depth of 10 μm . (c) Profilometric illustration of ring structure's well.

The test setup was validated with the use of an unstructured specimen and was proven to be able to accurately measure the viscosity in small gaps. Results are shown as mean values including standard deviations. As seen in Figure 4a the reproducibility of the measurements with distilled water at 20 °C was validated with an average dynamic viscosity of H₂O: $\eta = 1.07 \pm 0.08 \text{ mPas}$ which conforms to the values found in literature. Additionally, HA-enriched bovine serum as the SFS was measured on the reference specimen and the results show an average dynamic viscosity of SFS: $\eta = 35.4 \pm 0.7 \text{ mPas}$ at a constant shear rate of 100 s^{-1} , which is well within an acceptable mean variation. Investigating the impact of the proteins in the SFS, rheological measurements were carried out with and without HA-enrichment. The average apparent dynamic viscosity of the bovine serum without HA is very low (BS: $\eta' = 2.68 \pm 0.8 \text{ mPas}$), compared to the HA-enriched bovine serum (SFS: $\eta' = 39.2 \pm 0.7 \text{ mPas}$), as can be seen in Figure 4b.

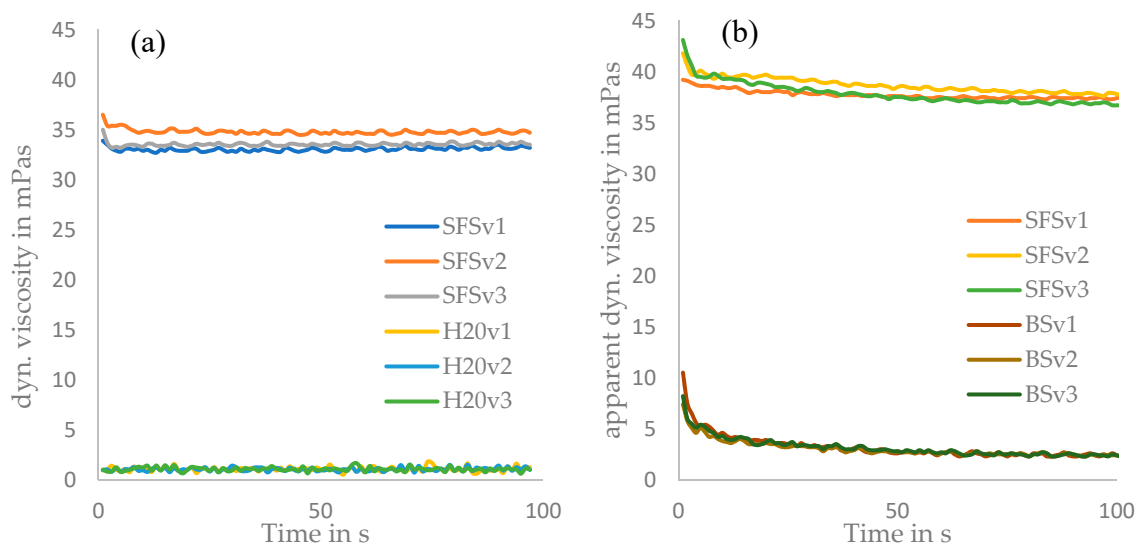


Figure 4. (a) Viscosity measurement of distilled water and hyaluronic acid (HA)-enriched synovial fluid substitute (SFS) on the unstructured reference specimen; (b) Comparison of the averaged viscosity measurement results of the synovial fluid substitute with and without HA enrichment on a microstructured sample (S2).

Rheological results have shown an overall increase in apparent dynamic viscosity of the synovial substitute with ring-like structures in comparison to a smooth surface, as seen in Figure 5. Differences in the microstructure such as width and depth resulting in different aspect ratios can be observed to have an impact as well. The change in aspect ratio leads to an increase in apparent dynamic viscosity in the range of 10% (S2: $\eta' = 39.2 \pm 1.8$ mPas) up to 20% (S9: $\eta' = 43.9 \pm 2.1$ mPas), compared to the smooth reference sample (Ref: $\eta = 35.4 \pm 0.7$ mPas). The change in texture area density leads to an increase in the range of 8% (S4: $\eta' = 38.4 \pm 0.9$ mPas) up to 30% (S6: $\eta' = 49.5 \pm 0.3$ mPas), compared to the smooth reference sample.

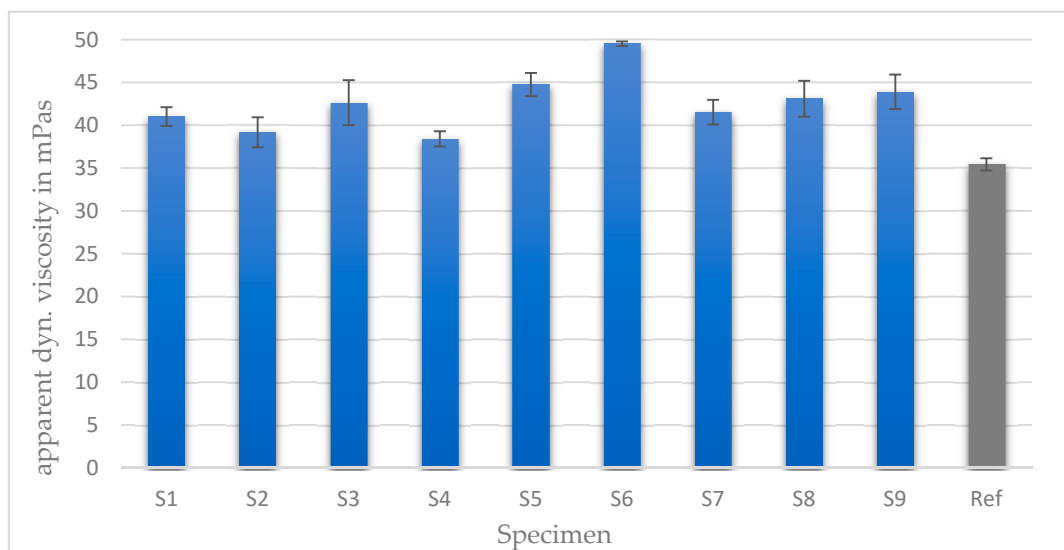


Figure 5. Overview of the average apparent dynamic viscosity of the synovia fluid substitute on various ring-like microstructures at 20 °C and a constant shear rate of 100 s⁻¹.

4. Discussion

As seen in Figure 4a, the effect of the proteins on the viscosity of the synovial fluid substitute is quite low and the synovial fluid substitute without HA does not represent the rheological properties of

normal SF or, in other words, the distinctive rheological behavior of SF is maintained by the hyaluronan content [21,23]. Therefore, the proteins in the bovine serum play a marginal role on the viscosity, compared to HA with both fluids showing a thixotropic behavior. This has also been observed in other studies that investigated the SF behavior of healthy and pathological human joints [24] as well as in the development of artificial synovial fluids [21,22]. The reason for the initial drop in viscosity is due to the thixotropic behavior of the SFS. In Figure 4a, the effect is less pronounced because the reference sample has no microstructure. In Figure 4b, the added microstructures lead to a stronger effect of the thixotropic behavior as well as the continuous decrease due to the non-Newtonian properties. Longer measurements result in a continuous decrease of the apparent dynamic viscosity until reaching approximately the same value as the unstructured reference specimen. This is probably because the microstructures are being filled with the proteins of the SFS.

Considering that the microstructures have different sizes, it is imperative to investigate and understand the main impact factors of the structures on the apparent dynamic viscosity, such as texture area density or aspect ratio. Qiu et al. recommended that the largest minimum lubricant film thickness in a knee bearing occurs with a texture area density of between 20% and 40% and an aspect ratio of 0.025 [10,13]. The microstructures in this study, however, consist of higher aspect ratios (0.33–1.33) and lower texture area densities (2%–10%) due to the geometric and space limitations of the ring structures. Ring-shaped microstructures have an advantage over many other geometries used in the aforementioned studies, due to their symmetry and, therefore, isotropic nature under friction. This study has shown that the apparent dynamic viscosity of the test fluid reaches much higher levels, with ring-shaped microstructures at texture area densities in the range of 2%–20%, than other structures such as net structures in the same area density range. This can be seen in a previous study where ring structures show the best results in comparison to various net structures or dimples [33]. The mechanics behind it are not yet fully understood. However, the symmetrical geometry of the ring structure can be regarded as a positive attribute and it could have an impact on the formation of a steadier lubricant film. This is because a reversal in flow direction and change in axis can retard, or even prevent the buildup of a protective protein surface layer [28]. Since hip endoprotheses are exposed to multi-axial movements, a symmetrical dimple or rather microstructure is basically favorable. Under a more thorough investigation in regard to texture area density and aspect ratio, it can be observed that higher texture densities are beneficial for an increase in apparent dynamic viscosity, as seen in Figure 6a. Lower aspect ratios have also been shown to have a positive effect on the dynamic viscosity of the test fluid but not to the extent as the texture area density, as seen in Figure 6b. The highest apparent dynamic viscosity of $\eta' = 49.5 \pm 0.3$ mPas was measured on specimen S6 which has the highest texture area density of 10.5%. The lowest viscosity on microstructured specimens was measured on the lowest texture area density of $\eta' = 38.4 \pm 0.9$ mPas, which shows that this parameter has a bigger impact, compared to the aspect ratio, as seen in Figure 6.

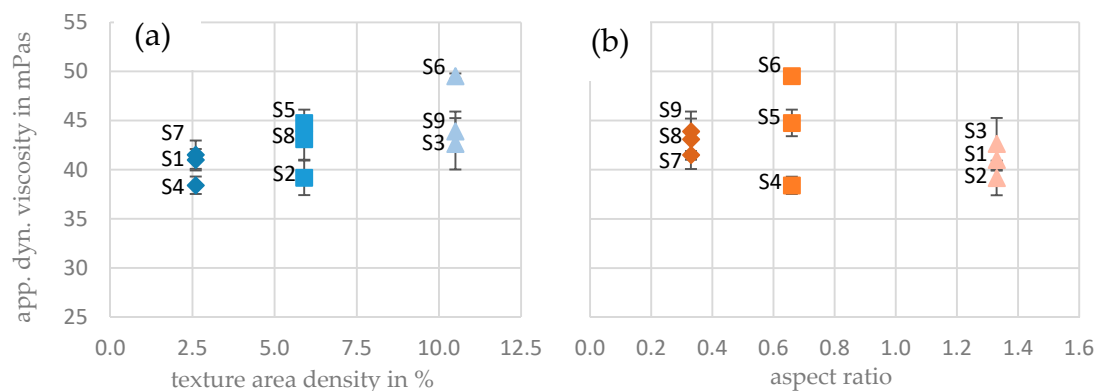


Figure 6. Correlation between texture area density (a) and aspect ratio (b) with the apparent dynamic viscosity of the non-Newtonian synovia substitute on different microstructures.

Contrary to this trend, the aspect ratio and the viscosity show only little correlation. In particular, the aspect ratio of 0.66 resulted in a large deviation between different microstructures. Why this particular aspect ratio shows such deviations is not yet understood but it could be due to the specific fluid interaction of the microstructures and the fluid. However, one could still argue that lower aspect ratios lead to higher viscosities in general. This can be seen in other studies that focused on the hydrodynamic pressure, coefficient of friction, or the film thickness of microstructures [11,13,37]. However, a direct correlation between film thickness and viscosity of the lubricant has not yet been determined. Further analysis with such different measurements can bring more insight.

The reason for higher apparent dynamic viscosities at microstructured surfaces in comparison to a smooth surface is the local change in gap size which results in a change in the shear rate of the fluid. The microstructures function as wells on surfaces that are a gap enlargement for the flow. The fluid can flow into the wells, lowering shear rates and increasing viscosity.

A high dynamic viscosity could lead to a better lubrication effect between the articulating joint surfaces. It is known that the viscosity of the synovial fluid is dependent on the pressure, shear rate and viscoelasticity of the synovial fluid. Even though the dynamic viscosity of the synovial fluid enters into the analysis of hydrodynamic, elasto-hydrodynamic, and elastorheodynamic lubrication, there is still no direct indication of a relationship between the viscosity and the viscoelastic properties [38]. In the hydrodynamic theory, the viscosity of the lubricant, the geometry, and velocities of the opposing surfaces are of importance [39]. However, it was concluded that neither the hydrodynamic theory nor the boundary theory permits an adequate description and explanation of lubrication in synovial joints [40]. This shows that there is still insufficient data to fully explain the mechanisms of lubrication in articulating synovial joints. A higher dynamic viscosity, due to added microstructures on the surface, can have an impact on the Stribeck curve, leading to a possible shift from the mixed lubrication to the hydrodynamic lubrication region and thus an increase and a more constant maintenance of the lubricant film thickness [41]. The pressure viscosity coefficient α is used for the calculation of lubricant film thickness. A study has postulated that whatever fundamental molecular properties govern the dynamic viscosity also causes proportional change in pressure viscosity coefficient [42].

Another possibility of higher dynamic viscosities at microstructured surfaces is the possible occurrence of cavitation and the corresponding pressure yields in the wells which could be responsible for the observed load support [43]. Although, it is unlikely that cavitation occurs at such low fluid flow velocities, it can therefore be considered improbable of being the likely cause of impacting the apparent dynamic viscosity in this test setup.

A higher hydrodynamic pressure mitigates the possibility of contact between the surfaces and, therefore, a reduction in friction. This can also be observed in studies that use hydrodynamic pressure as a medium for evaluating the reduction of friction [44,45]. An optimum in texture density is dependent not only by the texture geometry but also by the aspect ratio of the grooves [46]. A variance analysis with the two factors texture area density and aspect ratio ($n = 3$) was carried out. The texture area density of $p = 0.003$ shows highly statistical significance (significance level * $p > 0.05$, ** $p < 0.005$, *** $p < 0.001$) while the aspect ratio of $p = 0.2$ can be considered statistically insignificant.

The measurement of viscosity is a non-destructive and relatively fast process, compared to tribological tests. This new method can complement tribological tests determining the coefficient of friction, film thickness, and hydrodynamic pressure. Such tribological tests can be carried out by creating a Stribeck curve in order to get a deeper understanding about possible correlations. For example, a textured surface has an overall lower contact area, which may lead to a reduction of stiction [47]. Furthermore, an analysis of scratch marks or the amount of wear particles that are generated during such tests can give further insight on the improvement of friction due to microstructuring [3,18]. However, a study has observed that a structured surface texture may not be advantageous under fluid film lubrication, since the dimples may sometimes decrease the film thickness and result in asperity contacts [13].

This study has established a methodical foundation for investigating the lubricating effect of microstructures on implant surfaces by measuring the apparent dynamic viscosity and hence its corresponding lubrication properties. The impact of these microstructures in regard to tribological properties as well as mechanical properties such as bursting tests or wear resistance needs to be investigated. Furthermore, it would be of great importance to investigate the behavior of such microstructured surfaces with metal-on-plastic bearing pairs like CoCrMo-UHMWPE, which are used more frequently but show lower wear resistance, compared to hard-on-hard bearing pairs [18].

5. Conclusions

A synovial substitute fluid consisting of bovine serum and hyaluronic acid was developed in order to mimic the fluid properties of healthy human synovial fluid. The measurement of the apparent dynamic viscosity of the synovia substitute fluid was carried out successfully in a modified small gap parallel plate setup with specimens containing ring-shaped microstructured surfaces. The microstructures were created using a pulsed femtosecond laser with well-defined and sharp contours.

The specimens were rheologically measured with a reduced gap of 100 μm and a constant shear rate of 100 s^{-1} at room temperature.

The results of the rheological measurements show that ring-like microstructures have a significantly increasing effect on the apparent dynamic viscosity of the non-Newtonian synovial substitute fluid. It is hypothesized that this can improve lubrication and, therefore, lower the wear rate of the implant, resulting in a longer life cycle.

Microstructuring the surface via femtosecond laser leads to an increase in the measured viscosity of up to 39.8%. Variations of ring-like microstructures have given an insight into the impact of relevant parameters such as texture area density and aspect ratio. The highest value in apparent dynamic viscosity was reached at an aspect ratio of 0.66 and a texture area density of 10.9%.

A possible correlation between the friction coefficient, lubricant film thickness, hydrodynamic pressure and viscosity needs to be investigated to further understand the impact of microstructures on the lubrication performance of joint prostheses.

Author Contributions: The conceptualization of this study was carried out by P.D. and G.S.; sample preparation: P.O., P.D. and T.D.; methodology, investigation, validation, and formal analysis: P.D., P.O.; writing—original draft preparation: P.D.; writing—review and editing: G.S., P.O. and H.S.; supervision, H.S.; project administration, R.P. and H.S.; funding acquisition, R.P. and H.S. All authors have read and agreed to the published version of the manuscript.

Funding: This research was funded by the Federal Ministry of Education and Research (funding code: 03WKCU4B; Innovative Regional Growth Cores “MikroLas” which is part of the initiative “Entrepreneurial Regions”—“The BMBF Innovation Initiative for the New German Länder”). This work was supported by the German Research Foundation (DFG, grant number INST 264/133-1 FUGB. We also acknowledge financial support by the DFG and the University Rostock within the funding program Open Access Publishing.

Conflicts of Interest: The authors declare no conflict of interest. The funders had no role in the design of the study; in the collection, analyses, or interpretation of data; in the writing of the manuscript; or in the decision to publish the results.

References

1. Kung, M.S.; Markantonis, J.; Nelson, S.D.; Campbell, P. The Synovial Lining and Synovial Fluid Properties after Joint Arthroplasty. *Lubricants* **2015**, *3*, 394–412. [[CrossRef](#)]
2. Murray, D. Surgery and joint replacement for joint disease. *Acta Orthop. Scand.* **1998**, *69*, 17–20. [[CrossRef](#)] [[PubMed](#)]
3. Otto, M.; Kriegsmann, J.; Gehrke, T.; Bertz, S. Abriebpartikel: Schlüssel der aseptischen Prothesenlockerung? *Der Pathologe* **2006**, *27*, 447–460. [[CrossRef](#)] [[PubMed](#)]
4. Gachot, C.; Rosenkranz, A.; Hsu, S.; Costa, H. A critical assessment of surface texturing for friction and wear improvement. *Wear* **2017**, *372*, 21–41. [[CrossRef](#)]

5. Guo, L.; Wong, P.; Gachot, C. Facilitating the Study of the Texturing Effect on Hydrodynamic Lubrication. *Lubricants* **2018**, *6*, 18. [[CrossRef](#)]
6. Uddin, M.; Liu, Y.W. Design and optimization of a new geometric texture shape for the enhancement of hydrodynamic lubrication performance of parallel slider surfaces. *Biosurface Biotribol.* **2016**, *2*, 59–69. [[CrossRef](#)]
7. Gropper, D.; Wang, L.; Harvey, T.J. Hydrodynamic lubrication of textured surfaces: A review of modeling techniques and key findings. *Tribol. Int.* **2016**, *94*, 509–529. [[CrossRef](#)]
8. Wang, W.; He, Y.; Zhao, J.; Mao, J.; Hu, Y.; Luo, J. Optimization of groove texture profile to improve hydrodynamic lubrication performance: Theory and experiments. *Friction* **2018**, *8*, 83–94. [[CrossRef](#)]
9. Gachot, C.; Grützmacher, P.G.; Rosenkranz, A. Laser Surface Texturing of TiAl Multilayer Films—Effects of Microstructure and Topography on Friction and Wear. *Lubricants* **2018**, *6*, 36. [[CrossRef](#)]
10. Qiu, M.; Chyr, A.; Sanders, A.P.; Raeymaekers, B. Designing prosthetic knee joints with bio-inspired bearing surfaces. *Tribol. Int.* **2014**, *77*, 106–110. [[CrossRef](#)]
11. Chyr, A.; Qiu, M.; Speltz, J.W.; Jacobsen, R.L.; Sanders, A.P.; Raeymaekers, B. A patterned microtexture to reduce friction and increase longevity of prosthetic hip joints. *Wear* **2014**, *315*, 51–57. [[CrossRef](#)] [[PubMed](#)]
12. Borjali, A.; Langhorn, J.; Monson, K.; Raeymaekers, B. Using a patterned microtexture to reduce polyethylene wear in metal-on-polyethylene prosthetic bearing couples. *Wear* **2017**, *392*, 77–83. [[CrossRef](#)] [[PubMed](#)]
13. Gao, L.; Yang, P.; Dymond, I.; Fisher, J.; Jin, Z. Effect of surface texturing on the elastohydrodynamic lubrication analysis of metal-on-metal hip implants. *Tribol. Int.* **2010**, *43*, 1851–1860. [[CrossRef](#)]
14. Choudhury, D.; Rebenda, D.; Sasaki, S.; Hekrlé, P.; Vrbka, M.; Zou, M. Enhanced lubricant film formation through micro-dimpled hard-on-hard artificial hip joint: An in-situ observation of dimple shape effects. *J. Mech. Behav. Biomed. Mater.* **2018**, *81*, 120–129. [[CrossRef](#)]
15. Böhling, U.; Scholz, J.; Grundei, H.; Thomas, W. Bionische Oberflächengestaltung der Metall/Metall-Gleitpaarung in der Hüftendoprothetik Optimierung tribologischer Eigenschaften / Bionic surface design in metal on metal bearings for total hip arthroplasty—Optimization of tribological characteristics. *Biomed. Tech. Eng.* **2005**, *50*, 119–123. [[CrossRef](#)]
16. Cho, M.; Choi, H.-J. Optimization of Surface Texturing for Contact between Steel and Ultrahigh Molecular Weight Polyethylene Under Boundary Lubrication. *Tribol. Lett.* **2014**, *56*, 409–422. [[CrossRef](#)]
17. Langhorn, J.; Borjali, A.; Hippensteel, E.; Nelson, W.; Raeymaekers, B. Microtextured CoCrMo alloy for use in metal-on-polyethylene prosthetic joint bearings: Multi-directional wear and corrosion measurements. *Tribol. Int.* **2018**, *124*, 178–183. [[CrossRef](#)]
18. Sawano, H.; Warisawa, S.; Ishihara, S. Study on long life of artificial joints by investigating optimal sliding surface geometry for improvement in wear resistance. *Precis. Eng.* **2009**, *33*, 492–498. [[CrossRef](#)]
19. Tarabolsi, M.; Klassen, T.; Mantwill, F.; Gaertner, F.; Siegel, F.; Schulz, A.-P. Patterned CoCrMo and Al₂O₃ surfaces for reduced free wear debris in artificial joint arthroplasty. *J. Biomed. Mater. Res. Part A* **2013**, *101*, 3447–3456. [[CrossRef](#)]
20. Ito, H.; Kaneda, K.; Yuhta, T.; Nishimura, I.; Yasuda, K.; Matsuno, T. Reduction of polyethylene wear by concave dimples on the frictional surface in artificial hip joints. *J. Arthroplast.* **2000**, *15*, 332–338. [[CrossRef](#)]
21. Smith, A.; Fleming, L.; Wudebwe, U.; Bowen, J.; Grover, L.M. Development of a synovial fluid analogue with bio-relevant rheology for wear testing of orthopaedic implants. *J. Mech. Behav. Biomed. Mater.* **2014**, *32*, 177–184. [[CrossRef](#)] [[PubMed](#)]
22. Bortel, E.L.; Charbonnier, B.; Heuberger, R. Development of a Synthetic Synovial Fluid for Tribological Testing. *Lubricants* **2015**, *3*, 664–686. [[CrossRef](#)]
23. Nicholls, M.; Manjoo, A.; Shaw, P.; Niazi, F.; Rosen, J. A Comparison between Rheological Properties of Intra-articular Hyaluronic Acid Preparations and Reported Human Synovial Fluid. *Adv. Ther.* **2018**, *35*, 523–530. [[CrossRef](#)] [[PubMed](#)]
24. Johnston, J.P. The viscosity of normal and pathological human synovial fluids. *Biochem. J.* **1955**, *59*, 633–637. [[CrossRef](#)] [[PubMed](#)]
25. Mazzucco, D.; McKinley, G.H.; Scott, R.D.; Spector, M. Rheology of joint fluid in total knee arthroplasty patients. *J. Orthop. Res.* **2002**, *20*, 1157–1163. [[CrossRef](#)]
26. Jagatia, M.; Jin, Z.M. Elastohydrodynamic lubrication analysis of metal-on-metal hip prostheses under steady state entraining motion. *Proc. Inst. Mech. Eng. Part H J. Eng. Med.* **2001**, *215*, 531–541. [[CrossRef](#)] [[PubMed](#)]

27. Myant, C.; Cann, P. On the matter of synovial fluid lubrication: Implications for Metal-on-Metal hip tribology. *J. Mech. Behav. Biomed. Mater.* **2014**, *34*, 338–348. [[CrossRef](#)]
28. Myant, C.; Cann, P. The effect of transient conditions on synovial fluid protein aggregation lubrication. *J. Mech. Behav. Biomed. Mater.* **2014**, *34*, 349–357. [[CrossRef](#)]
29. Myant, C.; Underwood, R.; Fan, J.; Cann, P. Lubrication of metal-on-metal hip joints: The effect of protein content and load on film formation and wear. *J. Mech. Behav. Biomed. Mater.* **2012**, *6*, 30–40. [[CrossRef](#)]
30. Etsion, I. State of the Art in Laser Surface Texturing. *J. Tribol.* **2005**, *127*, 248–253. [[CrossRef](#)]
31. Chichkov, B.; Momma, C.; Nolte, S.; Alvensleben, F.; Tünnermann, A. Femtosecond, picosecond and nanosecond laser ablation of solids. *Appl. Phys. A* **1996**, *63*, 109–115. [[CrossRef](#)]
32. Raillard, B.; Mücklich, F. Ablation effects of femtosecond laser functionalization on surfaces. In *Laser Surface Engineering*; Elsevier: Oxford, UK, 2015; pp. 565–581.
33. Drescher, P.; Oldorf, P.; Dreier, T.; Peters, R.; Seitz, H. Modification of joint prosthesis surfaces by ultrashort pulse laser treatment for improved joint lubrication. *Curr. Dir. Biomed. Eng.* **2019**, *5*, 57–60. [[CrossRef](#)]
34. Wierschem, A.; Dakhil, H. Measuring low viscosities and high shear rates with a rotational rheometer in a thin-gap parallel-disk configuration. *Appl. Rheol.* **2014**, *24*. [[CrossRef](#)]
35. ISO 14242-1:2014. *Implants for Surgery-Wear of Total Hip-Joint Prostheses-Part 1: Loading and Displacement Parameters for Wear-Testing Machines and Corresponding Environmental Conditions for Test*. Available online: <https://www.iso.org/standard/63073.html> (accessed on 8 April 2020).
36. Balazs, E.A.; Watson, D.; Duff, I.F.; Roseman, S. Hyaluronic acid in synovial fluid. I. Molecular parameters of hyaluronic acid in normal and arthritic human fluids. *Arthritis Rheum.* **1967**, *10*, 357–376. [[CrossRef](#)]
37. Roy, T.; Choudhury, D.; Ghosh, S.; Bin Mamat, A.; Pinguang-Murphy, B. Improved friction and wear performance of micro dimpled ceramic-on-ceramic interface for hip joint arthroplasty. *Ceram. Int.* **2015**, *41*, 681–690. [[CrossRef](#)]
38. Thurston, G.B.; Greiling, H. Viscoelastic properties of pathological synovial fluids for a wide range of oscillatory shear rates and frequencies. *Rheol. Acta* **1978**, *17*, 433–445. [[CrossRef](#)]
39. Tanner, R.I. An Alternative Mechanism for the Lubrication of Synovial Joints. *Phys. Med. Boil.* **1966**, *11*, 119–127. [[CrossRef](#)]
40. Dintenfuss, L. Lubrication in Synovial Joints. *J. Bone Jt. Surgery-American Vol.* **1963**, *45*, 1241–1256. [[CrossRef](#)]
41. Braun, D.; Greiner, C.; Schneider, J.; Gumbsch, P. Efficiency of laser surface texturing in the reduction of friction under mixed lubrication. *Tribol. Int.* **2014**, *77*, 142–147. [[CrossRef](#)]
42. LaFountain, A.; Johnston, G.J.; Spikes, H.A. Elastohydrodynamic Friction Behavior of Polyalphaolefin Blends. In *Tribology Series*; Elsevier: Amsterdam, The Netherlands, 1998; Volume 34, pp. 465–475.
43. Hamilton, D.B.; Walowit, J.A.; Allen, C.M. A Theory of Lubrication by Microirregularities. *J. Basic Eng.* **1966**, *88*, 177–185. [[CrossRef](#)]
44. Tang, W.; Zhou, Y.; Zhu, H.; Yang, H. The effect of surface texturing on reducing the friction and wear of steel under lubricated sliding contact. *Appl. Surf. Sci.* **2013**, *273*, 199–204. [[CrossRef](#)]
45. Yu, H.; Wang, X.; Zhou, F. Geometric Shape Effects of Surface Texture on the Generation of Hydrodynamic Pressure between Conformal Contacting Surfaces. *Tribol. Lett.* **2009**, *37*, 123–130. [[CrossRef](#)]
46. Fesanghary, M.; Khonsari, M.M. On the optimum groove shapes for load-carrying capacity enhancement in parallel flat surface bearings: Theory and experiment. *Tribol. Int.* **2013**, *67*, 254–262. [[CrossRef](#)]
47. Wan, Y.; Xiong, D. The effect of laser surface texturing on frictional performance of face seal. *J. Mater. Process. Technol.* **2008**, *197*, 96–100. [[CrossRef](#)]

